Carbohydrate Polymers 90 (2012) 1235–1243

Contents lists available at SciVerse ScienceDirect

Carbohydrate Polymers

journal homepage: www.elsevier.com/locate/carbpol

Revisiting the conformation of xanthan and the effect of industrially relevant treatments

Syed K.H. Gulrez[a], Saphwan Al-Assaf[a,*], Yapeng Fang[a], Glyn O. Phillips[a,b], A. Patrick Gunning[a,c]

[a] Glyn O. Phillips Hydrocolloids Research Centre, Glyndwr University, Wrexham LL11 2AW, UK
[b] Phillips Hydrocolloid Research Ltd., 45 Old Bond Street, London W1S 4AQ, UK
[c] Institute of Food Research, Norwich Laboratory, Norwich Research Park, Colney, Norwich NR4 7UA, UK

ARTICLE INFO

Article history:
Received 3 April 2012
Received in revised form 20 June 2012
Accepted 21 June 2012
Available online 2 July 2012

Keywords:
Xanthan
Conformation
Molecular weight
Heating
Homogenisation
Autoclaving
Irradiation
AFM

ABSTRACT

The structure and conformation of xanthan in aqueous solution following various processing treatments typically encountered in its application were investigated in this study. Treatments such as heating, autoclaving, high pressure homogenisation and irradiation were subjected to the same sample. Parameters such as weight average molecular weight (M_w), polydispersity index, root mean square radius of gyration, intrinsic viscosity and Huggins constant were used to monitor the effect of these treatments. Additionally, we have quantified the mass recovery of samples examined by gel permeation chromatography and light scattering to properly account for all fractions present in xanthan solutions. Atomic force microscopy (AFM) images together with height measurements confirmed that xanthan conformation is double helical ordered renatured state (pre-heat treated by the manufacturer) in dilute solution conditions and random coil conformation in very dilute solution. The ordered (renatured) conformation is shown to have partially molten double helix, with more flexibility than the perfectly ordered native double helix. Heat treatment for 2 h at 85 °C reduces the M_w of xanthan to half its initial value, and mass recovery measurements indicate that it completely overcomes its associative nature. Thermally treated xanthan solution in the dilute region leads to an order–disorder transition, as determined by contour length per unit mass. Similarly, irradiation of xanthan solution results in an order–disorder transition together with the production of single strand low molecular weight molecules. Autoclaving and high pressure homogenisation treatments cause degradation of xanthan. The results from treated xanthan solutions following high pressure homogenisation and irradiation confirm that xanthan does not reassociate. A revised summary of xanthan conformation in solution together with schematic models following the various treatments are proposed.

1. Introduction

Xanthan is an extracellular hetero-polysaccharide produced by the bacterium xanthomonas campestris. It is an anionic polysaccharide with cellulose backbone (β-1–4)-D-glucose substituted at C3 on alternate glucose residues with a trisaccharide side chain (Morris, 2006). The noncarbohydrate substituents include O-acetate on the inner mannose residue and pyruvate on the terminal mannose residue. Different strains or fermentation conditions give rise to differing degrees of acetylation and pyruvylation, which moderate its functionality (Williams & Phillips, 2004). It is one of the major microbial polysaccharides employed in many industrial processes and often subjected to various processing conditions. Using X-ray diffraction, xanthan was shown to adopt a helical conformation having a five-fold symmetry and a pitch of 4.7 nm in the solid state (Moorhouse, Walkinshaw, & Arnott, 1976). However, in aqueous solution, xanthan undergoes an 'order' (helix) to 'disorder' (coil) transition depending on temperature, ionic strength and pH (Capron, Brigand, & Muller, 1997; Milas, Reed, & Printz, 1996), as well as on acetyl and pyruvate content (Morrison, Clark, Talashek, & Yuan, 2004; Smith, Symes, Lawson, & Morris, 1981). The ordered molecule of xanthan can undergo a conformational transition to a disordered flexible coil either by increasing the temperature above characteristic temperature (T_m) or by decreasing the salinity of solution (Callet, Milas, & Rinaudo, 1989; Capron et al., 1997; Capron, Yvon, & Muller, 1996; Gunning et al., 1998; Hacche, Washington, & Brant, 1987; Kawakami & Norisuye, 1991; Mehyar, Liu, & Han, 2008; Milas et al., 1996; Milas & Tinland, 1990; Oviatt & Brant, 1994b; Terada et al., 2005). T_m largely depends on concentration of the polymer and external salt (Rinaudo, 2001). The order–disorder conformational change (denaturation) of xanthan molecule in 0.01 M NaCl is reported at temperature near 50 °C (Capron et al., 1997). Within the ordered structure there exist two different kinds of conformation – native and renatured. Xanthan fermentation broth

* Corresponding author. Tel.: +44 (0)1978 29 3321; fax: +44 (0)1978 29 3370.
E-mail address: s.alassaf@glyndwr.ac.uk (S. Al-Assaf).

0144-8617/$ – see front matter © 2012 Elsevier Ltd. All rights reserved.
http://dx.doi.org/10.1016/j.carbpol.2012.06.055

without any heat treatment is reported to be in native state. Renatured xanthan can be obtained by heating the native form for few minutes at about 90 °C with immediate fast cooling (Callet, Milas, & Rinaudo, 1987; Capron et al., 1997; Milas et al., 1996). The renatured conformation is believed to be double helical with more flexibility than native conformation (Capron et al., 1997; Oviatt & Brant, 1994b). The disordered structure (denatured) is unanimously believed to be random coil and can be obtained by raising the temperature above T_m (>50 °C) while prolonged heating (>2 h) at high temperature results in degradation (Capron et al., 1997; Nishinari, Watase, Rinaudo, & Milas, 1996).

The stiffness of the xanthan polymer chain has been characterised by its persistence length L_p which is reported to be 5 nm, 45 nm and 125 nm for flexible random coil, single helix and rigid double helical conformations, respectively (Rinaudo, 2001). However, the strandedness of xanthan can be characterised by contour length M_L which is close to 1000 Dalton per nanometre (Da/nm) and 2000 Da/nm for single and double helix, respectively (Sato, Kojima, Norisuye, & Fujita, 1984; Sato, Norisuye, & Fujita, 1984).

Several treatments such as heating, autoclaving, microfluidising, etc. have been employed on polysaccharides including xanthan to overcome their associative nature and to promote conformational changes. Additionally, knowledge of the effect of these processes is beneficial for optimum performance of xanthan in various formulations. Capron et al. (1997) reported that the effect of heat treatment (110 °C for 20 min in 0.1 M NaCl) on xanthan conformation showed dissociation of the double helix into single strand i.e. denaturation (1997). Lagoueyte and Paquin (1998) showed that the process of microfluidisation (high pressure homogenisation) on xanthan solution caused degradation due to mechanical stress. Evidence for degradation was deduced from the continuous fall in the molecular weight and reduction in shear viscosity. Similar degradation effects following high pressure homogenisation of starch/amylopectin, methylcellulose and chitosan were reported by Modig, Nilsson, Bergenstahl, and Wahlund (2006), Floury, Desrumaux, Axelos, and Legrand (2002) and Kasaai, Charlet, Paquin, and Arul (2003), respectively. Autoclaving is another method used successfully to disperse aggregated molecules and thus reduce the associative nature of polysaccharides such as xyloglucan, oat β-glucan, and dextran in diluted solution (Wang, Wood, Cui, & Ross-Murphy, 2001). Following autoclaving, the degree of aggregation was found to be moderately reduced for xyloglucan and dextran whereas for oat β-glucan aggregation was significantly reduced based upon evidence from intrinsic viscosity and molecular weight distribution profiles.

The effect of high energy radiation, such as gamma ray and electron beam, on dilute polysaccharide solutions has been widely reported to result in degradation (Fei, Wach, Mitomo, Yoshii, & Kome, 2000). Free radicals, such as hydroxyl radical, hydrated electron and hydrogen atom, are generated from the radiolysis of water which randomly attack the polymer chain causing scission (Al-Assaf et al., 1995; Gulrez, Al-Assaf, & Phillips, 2011).

The precise structural details of the ordered conformation of xanthan remain a subject of debate, as two different models have been proposed. One group of researchers suggested a single stranded structure for ordered xanthan stabilised by alignment and packing of side chains along the polymer backbone. This hypothesis was based on light scattering, viscometry, sedimentation and concentration independence studies (Callet et al., 1987; Milas et al., 1996; Milas & Rinaudo, 1986; Milas & Tinland, 1990). On the other hand, the majority of studies have suggested a coaxial double helix for the ordered xanthan conformation (Brant, Hacche, & Washington, 1985; Capron et al., 1997; Gunning, Kirby, & Morris, 1996; Hacche et al., 1987; Hatakenaka, Liu, & Norisuye, 1987; Kawakami & Norisuye, 1991; Mehyar et al., 2008; Morrison et al., 2004; Oviatt & Brant, 1994a,b; Paradossi & Brant, 1982; Terada et al., 2005).

In this study, a commercial xanthan sample was subjected to different treatments in aqueous solution. These treatments were heating, autoclaving, high pressure homogenisation and radiation. Changes were monitored using light scattering and capillary viscometry. Crucially, in this study we quantified mass recovery on GPC-MALLS to properly characterise this heterogeneous system. Measurements based upon soluble fractions only cannot provide a full understanding of xanthan solution properties. Our objectives were: (i) to determine the corresponding effect on structural conformation in order to clarify some of the conflicting reports, (ii) to provide better understanding of how xanthan conformation could affect its functionality in various formulations and (iii) to examine whether xanthan order–disorder conformation is reversible following irradiation and autoclaving.

2. Materials and methods

A commercial xanthan sample (food grade, Lot No. 1394/FFA) in the powder form was kindly provided by Jungbunzlauer, Austria. Its pyruvate and acetyl contents were 6.3% and 2.2%, respectively. The sample has already been processed by the supplier to remove cell debris. Distilled water was used for the dispersion of xanthan and all reagents were of analytical grade obtained from Fisher Scientific, UK.

2.1. Loss on drying and solubility

The loss on drying was determined according to a method described previously (Al-Assaf, Phillips, Aoki, & Sasaki, 2007). The solubility was determined according to the following method. The weight (W_1) of a 70 mm glass fibre paper (pore size 1.2 μm) is determined following drying in a convection oven (Sanyo, MOV-212F) at 105 °C for 1 h and subsequently cooled in a desiccator containing silica gel. A dispersion was prepared by adding xanthan powder to distilled water to a concentration of 0.5 wt% (S) while stirring, followed by overnight hydration at room temperature. The hydrated dispersion was then centrifuged for 2–5 min at 2500 rpm prior to filtration. Drying of the filter paper was carried out in an oven at 105 °C followed by cooling to a constant weight (W_2). The percentage of insoluble material was calculated using:

$$\% \text{ insoluble} = \left(\frac{W_2 - W_1}{S}\right) * 100 \quad (1)$$

2.2. Solution preparation

An appropriate weight of xanthan was dissolved in distilled water and dispersed using a propeller type mixer at 200 rpm for 30 s. The solution was then left to hydrate overnight on a roller mixer. Appropriate dilution was then made in distilled water for the various treatments and measurements described below.

2.3. Heat treatment

Xanthan solutions at 4 mg ml^{-1} in distilled water were introduced into sealed ampoules with Teflon caps and immersed in water bath thermostated at 85 °C for different time periods (1–4 h). The solutions after the various treatments were stored at 4 °C until further use. Appropriate dilution was carried out for GPC-MALLS measurements.

2.4. Autoclaving

Xanthan solutions (4 mg ml^{-1}) were placed into sealed autoclave glass vials with metallic caps and placed into an autoclave

chamber. Autoclaving treatment was performed at 120 °C for 1–4 h (Model BSB040, Astell Scientific, UK). Depending on the duration, the whole treatment cycle (heating–stabilising–cooling) took nearly 2–5 h. The treated samples were cooled to room temperature, stored at 4 °C and used within 24 h of preparation. Appropriate dilution and sample pre-treatment (described in the relevant sections) were carried out for GPC-MALLS measurements.

2.5. High pressure homogenisation

Xanthan solutions at 4 mg ml^{-1} in distilled water were homogenised using a laboratory scale high pressure homogeniser (Nanomiser NM2-L100-D07, Collision type S generator, Yoshida Kikai Co. Ltd.). The solution was passed 3 times through the Nanomiser at each pressure condition and stored as described above for GPC-MALLS measurements.

2.6. Irradiation

A ^{137}Cs-gamma source supplied by Mainnance, UK (dose rate 36 Gy/h) was used to irradiate a xanthan solution at 4 mg ml^{-1} in distilled water: 10 ml were transferred to pyrex tubes, saturated with N_2O for 10 min and then sealed with glass stoppers. The solutions were then irradiated at dose levels of; 0.9, 1.8, 2.7, and 3.6 kGy. Gray (Gy) is defined as the absorption of 1 J of ionising radiation by 1 kg of matter. Under these conditions 90% of the radicals generated from radiolysis of the water are the highly oxidising hydroxyl radicals (Al-Assaf et al., 1995). Appropriate dilution was carried out for GPC-MALLS.

2.7. GPC-MALLS system

The GPC-MALLS system consisted of a degasser ERC-3215α (ERC, Japan), a constametric ® 3200 MS pump (Thermo Separation Products, FL), an injection valve with 100 μl loop (Reodyne 7725i) fitted inside a temperature regulated oven (Gilson, Model 831, UK) and a DAWN-DSP multi-angle light scattering photometer (Wyatt Technology, Santa Barbara, CA, USA) equipped with He–Ne laser (λ = 633 nm). Simultaneous concentration detection was performed using a calibrated differential refractometer (RI 2000, Schambek, Germany). A refractive index increment dn/dc value of 0.144 was used in the calculations (Capron et al., 1997). The mass recovery was obtained from the ratio of mass eluted from column (determined by integration of the refractometer signal) to the mass injected. The mobile phase was 0.1 M $LiNO_3$ containing 0.005% NaN_3 filtered through 0.2 μm pore size cellulose nitrate membrane. The samples injected were subjected to prior filtration through a nylon filter of 0.45 μm pore size. A set of two columns SB-803HQ and SB-806HQ (8 mm × 300 mm, Shodex OHpak, Japan, exclusion limits 1×10^5 and 2×10^7 g/mol) was used for the separation. The flow rate for the eluent was 0.45 ml/min. The Berry fitting method with linear fit was used for data processing in ASTRA software (Version 4.90.08). For the measurement of molecular weight, the solutions after the various treatments (autoclaving, high pressure homogenisation, and radiation) were further diluted into the range of 0.25–1 mg ml^{-1} and allowed to hydrate on a roller mixer for an additional 5 h. The solutions all contained the same molarity of buffer salt as the mobile phase. In the final preparation step the solutions were heated for 20 min at 60 °C and injected while hot. The entire GPC-MALLS system was maintained at 60 ± 1 °C. Temperature control was achieved using the in-house heating methodology provided thermostatic heating to all pipework between the detectors.

The well known expression for radius of gyration of a rigid rod polymer (Sato, Norisuye, et al., 1984) used in previous studies to determine the strandness of xanthan is given in following equation:

$$\left\langle S^2 \right\rangle^{1/2} = \frac{1}{\sqrt{12}} \left(\frac{M_w}{M_L} \right) \tag{2}$$

where $\left\langle S^2 \right\rangle^{1/2}$ is radius of gyration (R_g), M_w is molecular weight of polymer, M_L is molar mass per unit contour length of the rod. This can be obtained by plotting $M_w / \left(R_g * \sqrt{12} \right)$ on y-axis against M_w on x-axis and extrapolating to $M_w = 0$. At molecular weight approaching zero the polymer approximates a perfect rigid rod shape, while the intercept on y-axis will give the linear mass density for the polymer (Sato, Norisuye, et al., 1984).

2.8. Intrinsic viscosity

A calibrated Ubbelohde viscometer (Cannon Ubbelohde Semi-Micro Calib 75) was used to measure the flow time of solvent and solutions. Xanthan solution (at 4 mg ml^{-1}) was prepared in 0.1 M $LiNO_3$ solution containing 0.005% NaN_3. The solutions after various treatments were stored at 4 °C until further use. The viscometer was immersed in a water bath maintained at 60 ± 0.1 °C. The concentration of test solution was chosen such that for all these dilutions, the ratio of efflux time of solution to the solvent lies within the relative viscosity range of 2.2–1.2. All dilutions were made in situ. The efflux time at each dilution was measured in triplicate and the average was taken.

The intrinsic viscosity can be obtained by a double extrapolation to zero concentration using the combination of Huggins and Kraemer equations given below:

$$\frac{\eta_{sp}}{c} = [\eta] + k_1 [\eta]^2 c \tag{3}$$

$$\frac{In\eta_r}{c} = [\eta] - k_2 [\eta]^2 c \tag{4}$$

where η_r is the relative viscosity defined as the ratio of solution viscosity to solvent viscosity, and η_{sp} is the specific viscosity satisfying $\eta_{sp} = \eta_r - 1$. k_1 and k_2 are Huggins and Kraemer constants, respectively. The Kraemer constant k_2 is generally negative and smaller in magnitude than the Huggins constant k_1 (Huggins, 1942; Kraemer, 1938; Young & Shoemaker, 1991) and both are used to determine the quality of solvent.

The relationship of molecular weight to intrinsic viscosity and radius of gyration of a polymer is given by the Mark–Houwink–Kuhn–Sakurada formulae (Eqs. (5) and (6)). The coefficients 'a' and 'c' determine the conformation of the polymeric chain (Tombs & Hardings, 1998). For compact spherical conformation the value of 'c' is ~0.33 and for random coil it is in the range of 0.5–0.6, while at a 'c' value ~ 1.0, the conformation is rigid rod. Similarly, the value of 'a' for compact conformation is 0, and 0.5–0.8 for random coil and is 1.8 for a rigid rod conformation.

$$[\eta] = K' M^a \tag{5}$$

$$R_g = K'' M^c \tag{6}$$

2.9. Atomic force microscopy

Solutions of xanthan were prepared in distilled water according to the method described above. Additionally the solutions were heated at 60 °C for 20 min to ensure the complete dissolution and diluted to a final concentration of 10 μg ml^{-1}. Sample deposition took two forms. In the first, drops of the solution (5 μl) were applied to freshly cleaved mica surfaces, allowed to dry for about 10 min, and then imaged in air at room temperature. In the second, a modified mica surface was used. This was prepared by incubating freshly cleaved mica in a solution of poly-L-lysine (Sigma P8920)

at 10 μg ml^{-1} for 1 min followed by rinsing in ultrapure water and drying in a stream of argon. A 100 μl drop of the 10 μg ml^{-1} xanthan solution was incubated on a poly-L-lysine coated mica substrate for 1 min at room temperature, after which the surface was rinsed by dispensing ultrapure water (5× 1 ml) from a pipette. The sample was dried by blowing excess water off the mica with argon.

The atomic force microscope used in this study was an MFP-3D (Asylum Research, CA, USA) and was operated in the A/C control mode. The cantilevers used were Olympus AC160TS (Olympus, Japan) with a spring constant of around 42 N m^{-1} oscillated at a frequency 10% below resonance (typically around 320 kHz). The same probe was used to collect all of the images presented in this study. The damping set point for imaging was kept to the minimum value that allowed stable tracking of the sample surface to minimise any sample deformation. Images were acquired at a scan rate of 1 Hz.

3. Results and discussion

3.1. Conformation of xanthan

Fig. 1 shows a typical AFM image obtained on the sample prepared by drop deposition. The relatively linear appearance of the molecular chains seen in the image suggests that they are rigid. Height measurements indicate that the polymer chain height in thicker regions is 1.883 nm which is quite close to the helical diameter of xanthan (~2 nm) reported in literature (Gunning et al., 1996), while it is almost half (0.886 nm) in thinner regions suggesting the presence of molten double helical structure.

Fig. 2 shows a typical AFM image of the sample obtained following deposition of the dilute xanthan solution onto poly-L-lysine coated mica. The molecular chain is strikingly less pronounced in terms of height (0.178 nm) than those seen in Fig. 1 and, in addition, the sharp kinks along the chain suggest that it is significantly more flexible.

The deposition methodologies differ in two important respects: incubation of dilute xanthan solution onto poly-L-lysine coated mica will result in almost immediate electrostatic binding of the negatively charged xanthan molecules onto the positively charged poly-L-lysine layer, thus trapping the solution conformation of some of the molecules on the mica, and any remaining unbound molecules will be removed by the water rinse. Drop deposition, on the other hand, causes concentration of the xanthan solution as the solvent evaporates. Furthermore, the molecules are likely to remain mobile and hydrated until most of the water is lost, at which point the molecules finally become trapped on the mica surface by physisorption. The difference in the AFM images obtained using the different methods quite clearly point to conformational differences of the xanthan in the resulting molecular deposits. In the case of the drop deposited sample (Fig. 1) we propose that the molecular mobility coupled with the increasing concentration of the xanthan induces the renatured helical conformation once dried. The electrostatically bound xanthan molecules, such as the example presented in Fig. 2, appear to be trapped in the random coil conformation. This is consistent with the fact that they were bound to the surface from a very dilute solution of negligible ionic strength, where the coil conformation would be expected to predominate. Thus, the AFM images presented in Figs. 1 and 2 provide confirmation of the existence of two of xanthan's possible solution conformations.

3.2. Effects of heat treatment

The measurements to determine the weight average molecular weight (M_w), radius of gyration (R_g), mass recovery and polydispersity (M_w/M_n) were carried out at 60 °C to ensure aggregate free solutions. Similar measurements were previously reported at 25 °C by other researchers (Capron et al., 1997; Nishinari et al., 1996). Xanthan was shown not to lose its double strand suddenly at high temperature, but rather partial melting of the double helix.

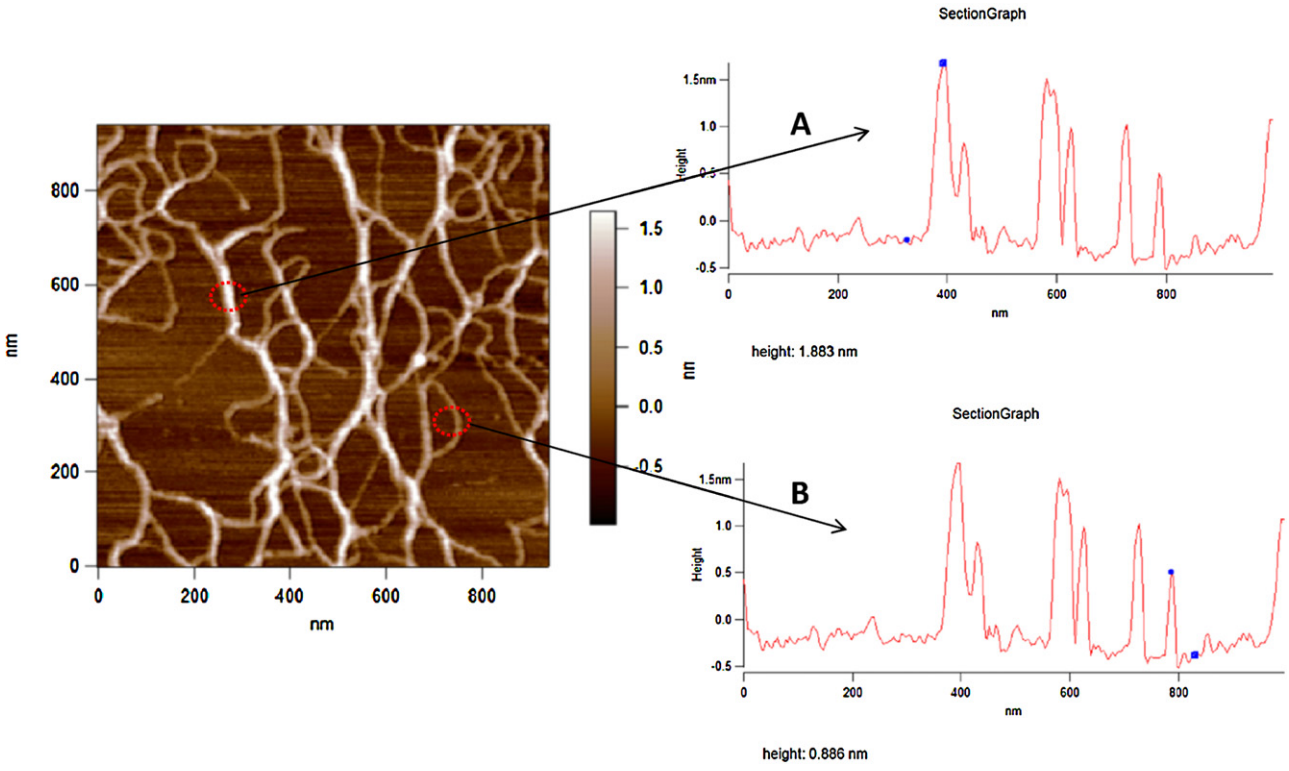

Fig. 1. Topography image of xanthan solution by AFM using A/C tapping mode and drop deposition method; height measurement of xanthan helices to determine strandedness in (A) thicker region and (B) thinner region.

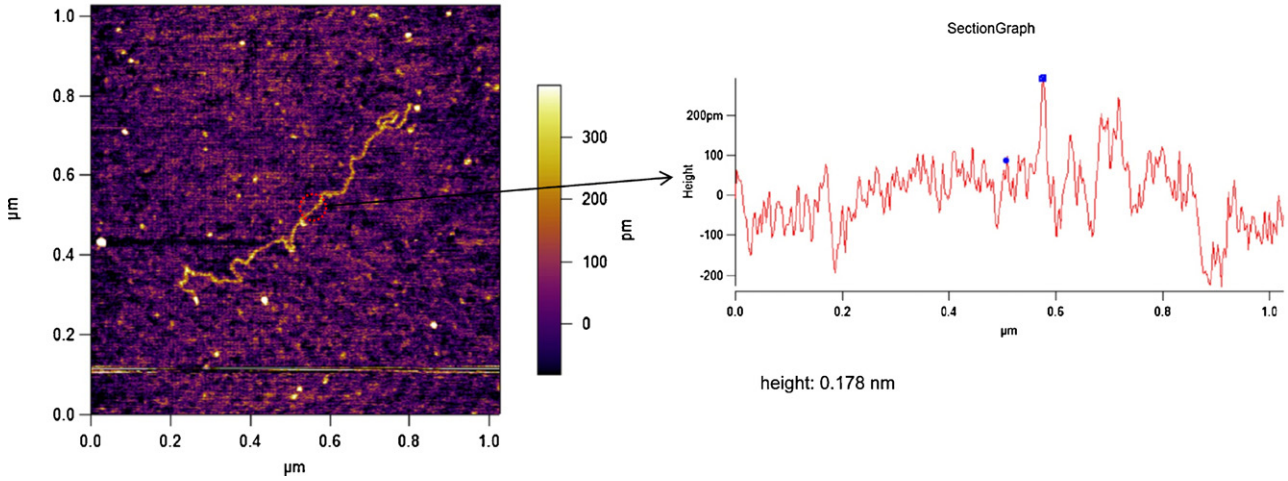

Fig. 2. AFM topography image of xanthan deposited onto poly-L-lysine coated mica; height measurement of the chain is used to determine molecular conformation.

Furthermore, previous studies also suggest that even after heating xanthan solution at 95 °C for 2.5 h, the dimer (double helical) fraction present is more than 60% (Kawakami & Norisuye, 1991; Mehyar et al., 2008). Based on these evidences, we do not expect to lose the strandedness of xanthan solution completely by measuring molecular weight at 60 °C (as the elution time is ~1 h in the GPC columns); nevertheless this temperature might have an effect on the flexibility of xanthan molecule in solution. Fig. 3 shows a typical elution profile monitored by the refractive index detector together with the molecular weight of each fraction plotted as a function of elution volume. No irregularity can be observed in the elution profile suggesting that the conditions are adequate for the smooth elution of high molecular weight fractions followed by low molecular weight.

The molecular weight for the solution heated for 20 min is given in Table 1 and the value obtained is consistent with previously reported values (Capron et al., 1997; Milas et al., 1996).

The mass recovery was 83% suggesting that ~17% of the mass was in the aggregated form and was retained on a 0.45 µm filter. Independent measurement to determine the solubility identified the presence of insoluble materials (aggregates) of nearly 8% in xanthan solution which was retained on a 1.2 µm filter. This suggests the disassociation (opening up) of aggregates present in xanthan solution following filtration through smaller pore size filters, and is consistent with results reported for hyaluronan (Al-Assaf, Phillips, Gunning, & Morris, 2002) and gum Arabic (Al-Assaf, Sakata, McKenna, Aoki, & Phillips, 2009). The intrinsic viscosity value (2.06 ml mg^{-1}) is similar to a previously reported value (Young & Shoemaker, 1991) and the Huggins constant value confirms good solvent condition (Higiro, Herald, Alavi, & Bean, 2007; Morris, 1995; Morris, Cutler, Ross-Murphy, & Rees, 1981). The effect of heat treatment (heating at 85 °C) was investigated as described above. Immediately after the heating cycle was completed, the hot

Table 1
GPC-MALLS parameters and intrinsic viscosity data for thermally treated xanthan solutions.

Time (min)	M^*10^{-5} (Da)	R_g (nm)	M_w/M_n	% Mass recovery	$[\eta]$ (ml mg^{-1})	k'
20	21.7	140	1.64	83	2.065	0.62
30	20.9	144	1.54	80	2.112	0.49
40	24.9	153	1.50	80	2.066	0.65
60	25.8	165	1.29	96	2.115	0.43
120	14.8	144	2.75	100	2.093	0.60

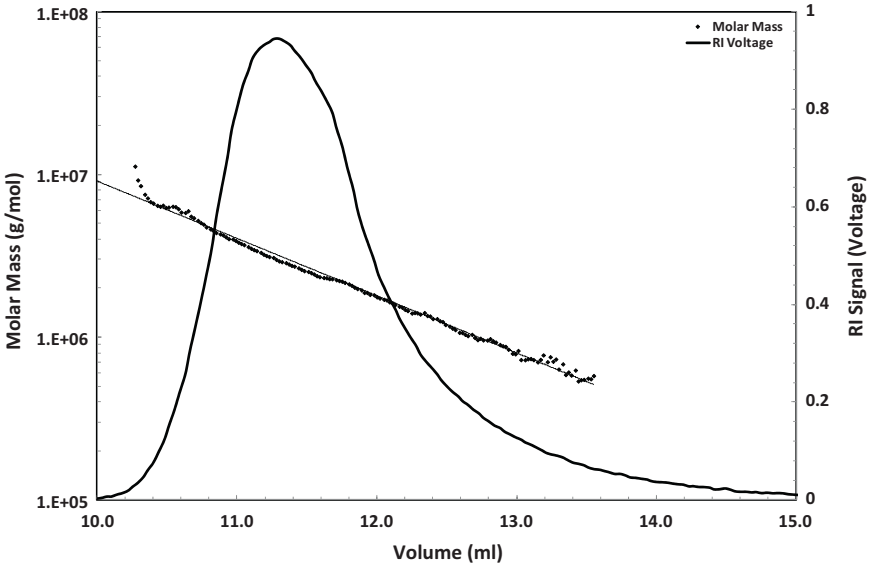

Fig. 3. Molecular weight versus elution volume and refractive index elution profile of xanthan. Injected at 0.25 mg ml^{-1} at the conditions described in Section 2.7.

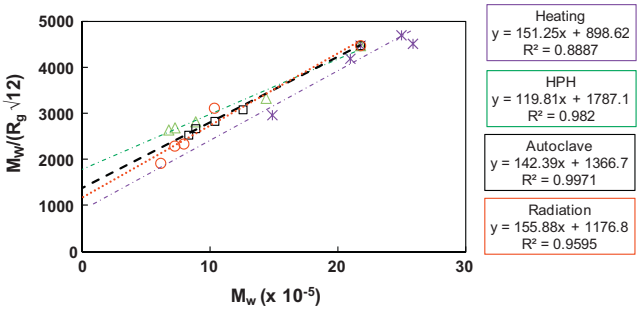

Fig. 4. Contour length (M_L) plotted as function of molecular weight for xanthan following (✳) heating; (△) high pressure homogenisation; (□) autoclaving; and (○) irradiation.

solution was injected into GPC-MALLS system. Heating for 30, 40 and 60 min gave comparable results with the exception of changes in the polydispersity and mass recovery. It is interesting to note that while there was no change in the molecular weight the mass recovery increased to 96% upon heating for 60 min and a lower polydispersity value was obtained. The reduction in the polydispersity value suggests disassociation of the high molecular weight aggregates to the extent where they can pass through a 0.45 μm filter. Further heating for 120 min shows a molecular weight reduction to nearly half the initial value of the 20 min heated sample, but with 100% mass recovery and the R_g value remains more or less unchanged. Capron et al. (1997) also reported the heat treatment of xanthan (30 min at 110 °C). Their results also showed a reduction of molecular weight to half the initial value without affecting R_g, and they attributed this change to dissociation of double helix into single strand. However, no information was provided on the polydispersity and mass recovery. In this study we provide further evidence of dissociation following heat treatment at 85 °C supported by the determination of the mass per unit length (M_L) value as shown in Fig. 4. A value of M_L for thermally treated xanthan was determined to be 904 Da/nm which is close to the value for single strand (1000 Da/nm) (Capron et al., 1997; Terada et al., 2005). The overall effect of heat treatment on xanthan solution could be summarised as dissociation of double helix into single strands as shown in Fig. 5.

Mark–Houwink Coefficients provide useful information concerning the conformational characteristics of polymer in solution. The slope of the curve obtained was ~0.7 (data not shown) which is less than the value (~1) for the perfectly rigid-rod double helical ordered native xanthan (Capron et al., 1997; Terada et al., 2005). The result indicates that the test material is in a double helical ordered form, with greater flexibility compared to native xanthan in agreement with AFM images shown in Fig. 1. Possible reasons for the slight variation from a perfect rigid-rod value could be due to the heat treatment and subsequent cooling or the underestimation of

Table 2
GPC-MALLS and viscometry data obtained for xanthan solutions following high pressure homogenisation treatment (3 passes at 25–100 MPa).

Treatment pressure (MPa)	$M_w * 10^{-5}$ (Da)	R_g (nm)	M_w/M_n	% Mass recovery	$[\eta]$ (ml mg^{-1})	k'
Control	21.7	140	1.64	83	2.06	0.73
25	14.31	124	1.57	86	1.39	0.63
50	8.80	90	1.25	86	0.94	0.41
75	7.18	77	1.42	85	0.78	0.34
100	6.69	73	1.31	91	0.75	nd

the intrinsic viscosity values determined by capillary viscometry. A previous study on cross-linked hyaluronan (hylan A) reported the major effect of shear rate applicable in the capillary viscosmeter compared to zero shear intrinsic viscosity obtained from a low shear rate Contraves rheometer (Al-Assaf et al., 2002). A value of 8.18 ml mg^{-1} was obtained from zero shear rate viscosity measurements compared to a value of 5.14 ml mg^{-1} using a capillary viscometer.

3.3. Effects of high pressure homogenisation

Xanthan solution at 4 mg ml^{-1} was subjected to high pressure homogenisation treatments at 25, 50, 75 and 100 MPa in order to reduce its associative nature. The solution (4 mg ml^{-1}) was passed through the homogeniser three times and was further diluted to 0.25 mg ml^{-1} for GPC-MALLS measurements. Its intrinsic viscosity was also measured at 60 °C to correlate with light-scattering data. The values obtained are presented in Table 2.

Table 2 shows a continuous fall in M_w, R_g, polydispersity and $[\eta]$ which indicates degradation of xanthan by high pressure homogenisation. The results further support the findings of a previous study on xanthan which reported polymer degradation due to mechanical stress, using reduction in molecular weight as the only evidence (Lagoueyte & Paquin, 1998). The results given in Table 2 also show a clear trend in increasing the mass recovery as a function of the applied total pressure. However, we found no evidence for dissociation of xanthan polymer chains (double strand to single strand), as M_L remains ~2000 Da/nm (Fig. 4). The results given in Table 2 are summarised schematically in Fig. 6 where the renatured xanthan is degraded into smaller molecules, but retains its double helical conformation.

Conformational changes in xanthan solutions subjected to elevated temperatures are reported to be permanent and no reassociation takes place, once the dissociation has occurred. This has been shown by Capron et al. (1997) by comparing the molecular weight of a sample obtained by injecting immediately after heat treatment, with that of the same sample stored at 4 °C and injected the following day. In this study similar measurements were performed to show that conformational changes due to high

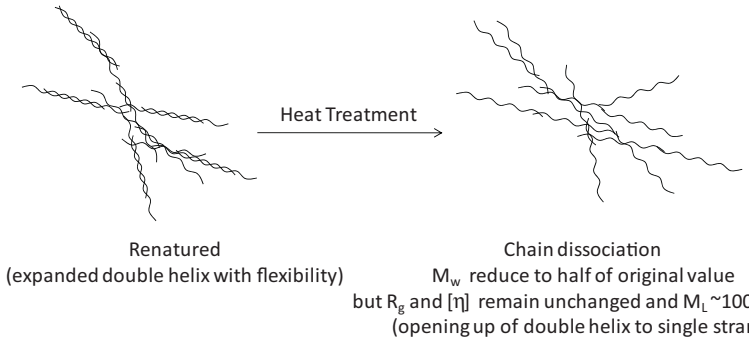

Fig. 5. Schematic illustration of structural and conformational changes in a commercial xanthan sample due to effect of heat treatment.

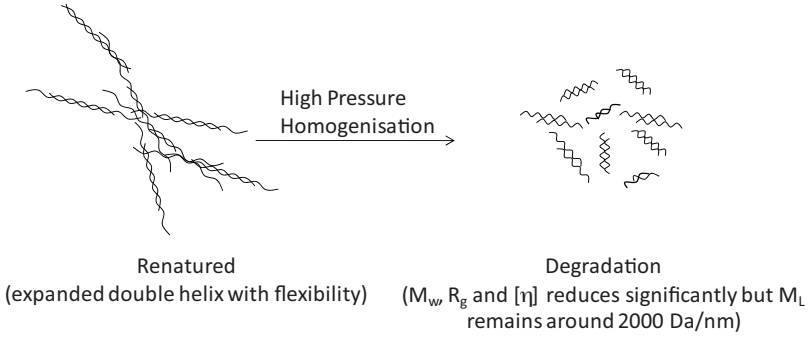

Fig. 6. Schematic illustration of structural and conformational changes in xanthan aqueous solution following high pressure homogenisation.

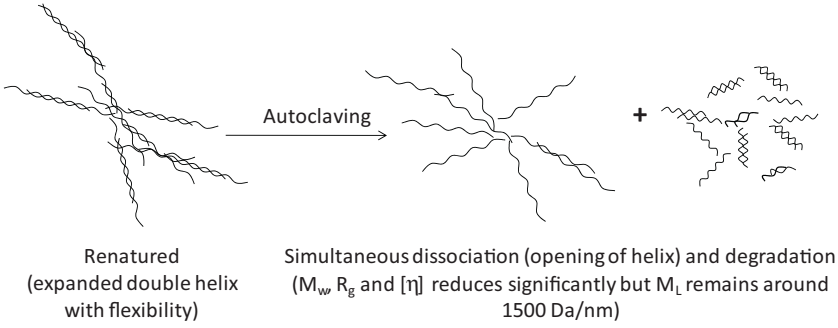

Fig. 7. Schematic illustration of structural and conformational changes in xanthan aqueous solution due to effect of autoclaving at 120 °C. Condition described in Section 2.4.

pressure treatments on xanthan solution are permanent and time-independent. In order to demonstrate this effect, a high pressure homogenised solution (50 MPa, 3 passes) was stored at 4 °C for 3 days and re-injected into GPC-MALLS to investigate any conformational changes. The results showed a slight reduction in M_w from 8.80×10^6 to 8.6×10^6 g/mol while R_g, polydispersity and mass recovery remained unchanged. This suggests that the dissociation induced by high pressure treatment is irreversible and xanthan molecules, albeit in double strand form, do not reassociate upon storage at 4 °C.

Table 3
GPC-MALLS and viscometry data obtained for xanthan solution after autoclaving (120 °C, 1–4 h).

Autoclave time (h)	$M_w * 10^{-5}$ (Da)	R_g (nm)	M_w/M_n	% Mass recovery	$[\eta]$ (ml mg^{-1})	k'
Control	21.7	140	1.64	83	2.06	0.73
1	12.5	117	1.31	89	1.61	0.54
2	10.3	105	1.40	92	1.36	0.49
3	8.8	95	1.16	95	1.27	0.35
4	8.2	94	1.28	96	0.90	0.51

Table 4
GPC-MALLS and viscometry data obtained for dilute xanthan solutions (4 mg ml^{-1}) following irradiation treatments.

Radiation dose (kGy)	$M_w * 10^{-5}$ (Da)	R_g (nm)	M_w/M_n	% Mass recovery	$[\eta]$ (ml mg^{-1})	k'
Control	21.7	140	1.64	83	2.06	0.73
0.9	10.26	95	2.03	80	1.78	0.55
1.8	7.87	97	2.29	86	1.48	0.53
2.7	7.16	90	2.33	96	1.47	0.64
3.6	6.06	91	2.50	100	1.10	0.56

3.4. Effects of autoclaving

The molecular weight parameters, intrinsic viscosity and Huggins constant of control and autoclaved xanthan solutions are given in Table 3. A contour plot to determine the conformation of the material is shown in Fig. 4.

The autoclaving effect shows a continuous reduction in molecular weight, R_g as well as intrinsic viscosity (Table 3). It demonstrates that the effect of autoclaving on xanthan is similar to the degradation seen on oat β-glucan in the study by Wang et al. (2001). However, the linear mass density calculated for autoclaved

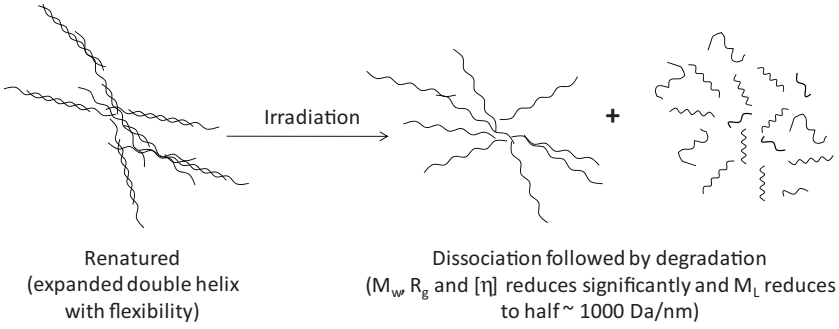

Fig. 8. Schematic illustration of structural and conformational changes in xanthan following irradiation in dilute aqueous solution.

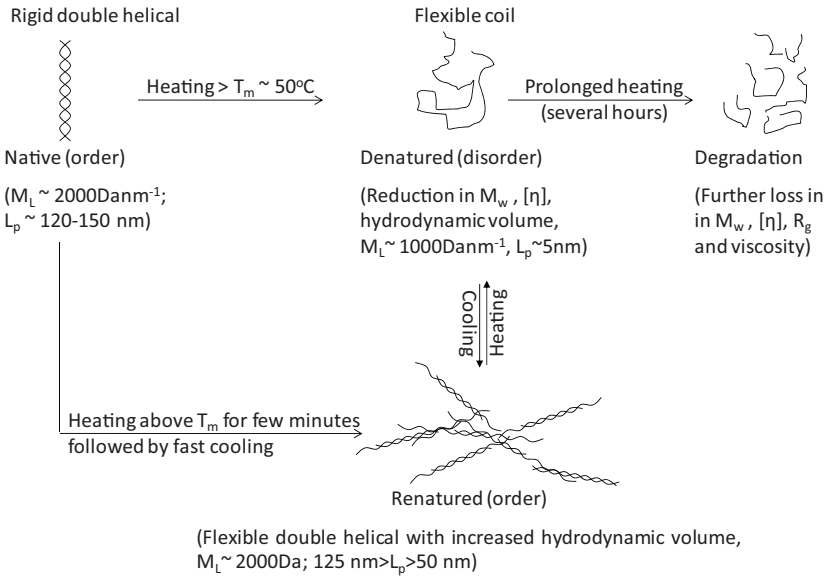

Fig. 9. Schematic representation summarising the order–disorder conformation of xanthan in aqueous solution reported in the literature. References as given in Section 1.

xanthan shows a value of ~1500 Da/nm (Fig. 4), which lies between the values for single strand (1000) and double strands (2000). So, it can be suggested that dissociation (due to high temperature) and degradation (due to high pressure) both occur simultaneously in xanthan solutions which are autoclaved. The results given in Table 3 are summarised schematically in Fig. 7 where both degradation and dissociation of the renatured xanthan chains occur.

3.5. Effects of irradiation in dilute solution

Xanthan was irradiated in diluted state (4 mg ml^{-1}, solution saturated in N_2O) and further characterised by light scattering and viscometry. The results showed a reduction in molecular weight, intrinsic viscosity as well as R_g values (Table 4). This indicates that irradiation of diluted solution results in degradation due to the generation of hydroxyl radicals (resulting from water radiolysis). These radicals randomly attack the polymer chains and lead to chain scission (Fei et al., 2000). The generation of radicals and the energy delivered by the radiation might also affect the association of xanthan molecules, depending on the radiation dose and may lead to order–disorder transition. It is interesting to note that there was an increase in the polydispersity as a function of increasing the irradiation dose, consistent with a random attack mechanism on xanthan molecules. Furthermore, there was also an increase in the mass recovery, and at the highest radiation dose the value obtained suggests the complete dispersal of aggregates.

Further evidence for a radiation-induced order–disorder transition was obtained by linear mass density calculation. The M_L value for an irradiated dilute xanthan solution is ~1173 Da/nm (Fig. 4) which is close to the value for single strand. These results indicate that irradiation of xanthan in dilute solution leads to an order–disorder transition (dissociation followed by degradation). The overall effect of radiation on dilute xanthan solution could be summarised as in situ dissociation followed by degradation (Fig. 8).

To demonstrate that radiation-induced conformational changes of xanthan solution are permanent and time-independent, an irradiated solution (900 Gy dose) was stored at 4 °C for 7 days and re-injected into GPC-MALLS. The data obtained are shown in Table 5 which demonstrates that the dissociation induced by such treatments is irreversible and xanthan molecules do not reassociate with time upon storage at 4 °C.

Table 5
Molecular weight parameters for irradiated xanthan in aqueous solution and following storage for one week at 4 °C.

Treatment	Dose	$M_w * 10^{-5}$ (Da)	R_g (nm)	M_w/M_n	% Mass recovery
Radiation	900 Gy	10.26	95	2.03	80
	After one week	10.10	98	2.07	80

4. Conclusion

Different treatments such as heating and ultrasonification have been applied to xanthan solutions in the past to break the molecular associations, but the precise changes induced by such treatments remain obscure. This is the first comprehensive study to apply different treatments (homogenisation, autoclaving, heat treatment and irradiation) on the same sample. Optimum conditions for GPC-MALLS have been demonstrated, yielding physical data on the molecular state of xanthan in solution that should be more reliable. Based on AFM, M_w, R_g, [η], Mark–Houwink coefficient c and M_L data we have confirmed that the test material is double helical ordered renatured state. Together with the results obtained in this study and those reported previously it is now possible to reconcile the two conflicting reports about xanthan conformation as shown in the scheme presented in Fig. 9. Subsequently, the resulting conformations are proposed following each treatment based on the model given in Fig. 9. This work provides a rational basis for the manipulation of xanthan to overcome the barrier of its associative nature and aggregation. Furthermore, the effect of these treatments on xanthan conformation will also be useful to understand its synergetic interaction with other polysaccharides, particularly galactomannans. Finally, the study reveals how a series of low molecular weight xanthan fractions with tuneable conformations can be produced through the knowledge-led application of the treatments described herein.

References

Al-Assaf, S., Phillips, G. O., Aoki, H., & Sasaki, Y. (2007). Characterization and properties of *Acacia senegal* (L.) Willd. var. *senegal* with enhanced properties (*Acacia* (sen) SUPER GUM(TM)). Part 1. Controlled maturation of *Acacia senegal* var.

senegal to increase viscoelasticity, produce a hydrogel form and convert a poor into a good emulsifier. *Food Hydrocolloids*, *21*(3), 319–328.
Al-Assaf, S., Phillips, G. O., Deeble, D. J., Parsons, B., Starnes, H., & Von Sonntag, C. (1995). The enhanced stability of the cross-linked hylan structure to hydroxyl (OH) radicals compared with the uncross-linked hyaluronan. *Radiation Physics and Chemistry*, *46*(2), 207–217.
Al-Assaf, S., Phillips, G. O., Gunning, A. P., & Morris, V. J. (2002). Molecular interaction studies of the hyaluronan derivative, hylan A using atomic force microscopy. *Carbohydrate Polymers*, *47*(4), 341–345.
Al-Assaf, S., Sakata, M., McKenna, C., Aoki, H., & Phillips, G. O. (2009). Molecular associations in acacia gums. *Structural Chemistry*, *20*, 325–336.
Brant, D. A., Hacche, L. S., & Washington, G. E. (1985). A light-scattering study of the temperature-driven conformation change in xanthan. *Abstracts of Papers of the American Chemical Society*, *190*(SEP), 86-MBD.
Callet, F., Milas, M., & Rinaudo, M. (1987). Influence of acetyl and pyruvate contents on rheological properties of xanthan in dilute-solution. *International Journal of Biological Macromolecules*, *9*(5), 291–293.
Callet, F., Milas, M., & Rinaudo, M. (1989). On the role of thermal treatments on the properties of xanthan solutions. *Carbohydrate Polymers*, *11*(2), 127–137.
Capron, I., Brigand, G., & Muller, G. (1997). About the native and renatured conformation of xanthan exopolysaccharide. *Polymer*, *38*(21), 5289–5295.
Capron, I., Yvon, M., & Muller, G. (1996). In vitro gastric stability of carrageenan. *Food Hydrocolloids*, *10*(2), 239–244.
Fei, B., wach, R. A., Mitomo, H., Yoshii, F., & Kome, T. (2000). Hydrogel of biodegradable cellulose derivatives. I. Radiation-induced crosslinking of CMC. *Journal of Applied Polymer Science*, *78*, 278–283.
Floury, J., Desrumaux, A., Axelos, M. A. V., & Legrand, J. (2002). Degradation of methylcellulose during ultra-high pressure homogenisation. *Food Hydrocolloids*, *16*(1), 47–53.
Gulrez, S. K. H., Al-Assaf, S., & Phillips, G. O. (2011). Hydrogels: Methods of preparation, characterisation and applications. In A. Carpi (Ed.), *Progress in molecular and environmental bioengineering – From analysis and modeling to technology applications*.. In Tech.
Gunning, A. P., Cairns, P., Kirby, A. R., Round, A. N., Bixler, H. J., & Morris, V. J. (1998). Characterising semi-refined iota-carrageenan networks by atomic force microscopy. *Carbohydrate Polymers*, *36*(1), 67–72.
Gunning, A. P., Kirby, A. R., & Morris, V. J. (1996). Imaging xanthan gum in air by ac tapping mode atomic force microscopy. *Ultramicroscopy*, *63*, 1–3.
Hacche, L. S., Washington, G. E., & Brant, D. A. (1987). Light-scattering investigation of the temperature-driven conformation change in xanthan. *Macromolecules*, *20*(9), 2179–2187.
Hatakenaka, K., Liu, W., & Norisuye, T. (1987). Stability of xanthan in aqueous sodium-chloride at elevated-temperature. *International Journal of Biological Macromolecules*, *9*(6), 346–348.
Higiro, J., Herald, T. J., Alavi, S., & Bean, S. (2007). Rheological study of xanthan and locust bean gum interaction in dilute solution: Effect of salt. *Food Research International*, *40*(4), 435–447.
Huggins, M. L. (1942). The viscosity of dilute solutions of long-chain molecules. 4. Dependence on concentration. *Journal of the American Chemical Society*, *64*, 2716–2718.
Kasaai, M. R., Charlet, G., Paquin, P., & Arul, J. (2003). Fragmentation of chitosan by microfluidization process. *Innovative Food Science & Emerging Technologies*, *4*, 403–413.
Kawakami, K., & Norisuye, T. (1991). 2nd virial-coefficient for charged rods – Sodium xanthan in aqueous sodium-chloride. *Macromolecules*, *24*(17), 4898–4903.
Kraemer, E. O. (1938). Molecular weight of cellulose and cellulose derivatives. *Industrial and Engineering Chemistry*, *30*, 1200–1203.
Lagoueyte, N., & Paquin, P. (1998). Effects of microfluidization on the functional properties of xanthan gum. *Food Hydrocolloids*, *12*(3), 365–371.
Mehyar, G. F., Liu, Z., & Han, J. H. (2008). Dynamics of antimicrobial hydrogels in physiological saline. *Carbohydrate Polymers*, *74*, 92–98.
Milas, M., Reed, W. F., & Printz, S. (1996). Conformation and flexibility of native and re-natured xanthan in aqueous solutions. *International Journal of Biological Macromolecules*, *18*, 211–221.
Milas, M., & Rinaudo, M. (1986). Properties of xanthan gum in aqueous-solutions – Role of the conformational transition. *Carbohydrate Research*, *158*, 191–204.
Milas, M., & Tinland, B. (1990). Behaviour of xanthan in cadoxen. *Carbohydrate Polymers*, *13*, 47–56.
Modig, G., Nilsson, L., Bergenstahl, B., & Wahlund, K.-G. (2006). Homogenization-induced degradation of hydrophobically modified starch determined by asymmetrical flow field-flow fractionation and multi-angle light scattering. *Food Hydrocolloids*, *20*, 1087–1095.
Moorhouse, R., Walkinshaw, M. D., & Arnott, S. (1976). Xanthan gum molecular conformation and interactions. *Abstracts of Papers of the American Chemical Society*, *172*(SEP3), 20.
Morris, E. R. (Ed.). (1995). *Polysaccharide rheology and in-mouth perception*.. New York: Marcel Dekker.
Morris, E. R., Cutler, A. N., Ross-Murphy, S. B., & Rees, D. A. (1981). Concentration and shear rate dependence of viscosity in random coil polysaccharide solutions. *Carbohydrate Polymers*, *1*, 5–21.
Morris, V. J. (2006). Bacterial polysaccharides. In A. M. Stephen, G. O. Phillips, & P. A. Williams (Eds.), *Foood polysaccharides and their applications* (pp. 413–454). London: Taylor & Francis.
Morrison, N. A., Clark, R., Talashek, T., & Yuan, C. R. (2004). New forms of xanthan gum with enhanced properties. *Gums and Stabilizers for the Food Industry*, *12*(294), 124–130.
Nishinari, K., Watase, M., Rinaudo, M., & Milas, M. (1996). Characterization and properties of gellan-kappa-carrageenan mixed gels. *Food Hydrocolloids*, *10*(3), 277–283.
Oviatt, H. W., & Brant, D. A. (1994a). The rheological behavior of semidilute aqueous xanthan solutions after thermal-treatment. *Abstracts of Papers of the American Chemical Society*, *207*, 394–400.
Oviatt, H. W., & Brant, D. A. (1994b). Viscoelastic behavior of thermally treated aqueous xanthan solutions in the semidilute concentration regime. *Macromolecules*, *27*(9), 2402–2408.
Paradossi, G., & Brant, D. A. (1982). Light-scattering study of a series of xanthan fractions in aqueous-solution. *Macromolecules*, *15*(3), 874–879.
Rinaudo, M. (2001). Relation between the molecular structure of some polysaccharides and original properties in sol and gel states. *Food Hydrocolloids*, *15*(4–6), 433–440.
Sato, T., Kojima, S., Norisuye, T., & Fujita, H. (1984). Double-stranded helix of xanthan in dilute-solution – Further evidence. *Polymer Journal*, *16*(5), 423–429.
Sato, T., Norisuye, T., & Fujita, H. (1984). Double-stranded helix of xanthan in dilute-solution – Evidence from light-scattering. *Polymer Journal*, *16*(4), 341–350.
Smith, I. H., Symes, K. C., Lawson, C. J., & Morris, E. R. (1981). Influence of the pyruvate content of xanthan on macromolecular association in solution. *International Journal of Biological Macromolecules*, *3*(2), 129–134.
Terada, S., Yoshimoto, H., Fuchs, J. R., Sato, M., Pomerantseva, I., Selig, M. K., et al. (2005). Hydrogel optimization for cultured elastic chondrocytes seeded onto a polyglycolic acid scaffold. *Journal of Biomedical Materials Research Part A*, *75A*(4), 907–916.
Tombs, M. P., & Hardings, S. E. (1998). *An introduction to polysaccharide biotechnology*. London: Taylor & Francis Press.
Wang, Q., Wood, P. J., Cui, W., & Ross-Murphy, S. B. (2001). The effect of autoclaving on the dispersibility and stability of three neutral polysaccharides in dilute aqueous solutions. *Carbohydrate Polymers*, *45*(4), 355–362.
Williams, P. A., & Phillips, G. O. (2004). Introduction to food hydrocolloid. In G. O. Phillips, & P. A. Williams (Eds.), *Handbook of hydrocolloid* (pp. 1–19). Cambridge, UK: Woodhead Publication.
Young, S. L., & Shoemaker, C. F. (1991). Measurement of shear-dependent intrinsic viscosities of carboxymethyl cellulose and xanthan gum suspensions. *Journal of Applied Polymer Science*, *42*(9), 2405–2408.